Supplementary Information

The synthesis and characterization of Zn(II)/Cd(II) based MOFs by a mixed ligand strategy: a Zn(II) MOF as a dual functional material for reversible dye adsorption and as a heterogeneous catalyst for the Biginelli reaction

Unnati Patel,[a] Bhavesh Parmar,[b,c] Parth Patel,[a,d] Abhishek Dadhania,[a,b*] and Eringathodi Suresh[b,c*]

[a]Department of Chemical Sciences, P. D. Patel Institute of Applied Sciences, Charotar University of Science and Technology, Changa-388 421, Gujarat, India.

[b]Analytical and Environmental Science Division and Centralized Instrument Facility, CSIR–Central Salt and Marine Chemicals Research Institute, G. B. Marg, Bhavnagar-364 002, Gujarat, India.

[c]Academy of Scientific and Innovative Research (AcSIR), Ghaziabad-201 002, India.

[d]Inorganic Materials and Catalysis Division, CSIR-Central Salt and Marine Chemicals Research Institute, G. B. Marg, Bhavnagar-364 002, Gujarat, India.

E-mail: abhishekdadhania.bt@charusat.ac.in ; esuresh@csmcri.res.in

Experimental Section

Materials and General Methods

All reagents and solvents were purchased from commercial sources and were used as received without any purification. Distilled water was used for synthetic manipulations. N-donor, (E)-N'-(pyridin-3-ylmethylene)nicotinohydrazide (**L**) was synthesized according to our previous report.[S1] CHNS analysis was done using an Elementar Vario MICRO CUBE analyzer. FT-IR spectra were recorded on a Thermo Nicolet 6700 spectrophotometer using KBr pellet method. ^{1}H NMR and ^{13}C NMR spectra were recorded on a JEOL, JNM-ECZ 600R (600 MHz) and Bruker, Avance II 500 (500 MHz) spectrometer using DMSO-d_6/$CDCl_3$ as a solvent with respect to TMS as internal

reference. TG analysis were performed on Mettler Toledo thermal analyzer under nitrogen environment with a heating rate at 10 °C/min. Powder X-ray diffraction (PXRD) data were collected using a Bruker, D2 phaser bench-top diffractometer and crystal structures of the MOF were determined using a Bruker D8 QUEST diffractometer. The BET surface area was measured on a Micromeritics, 3 Flex instrument. Liquid and solid-state UV−Vis spectra were recorded using a Shimadzu UV-Visible Spectrophotometer (UV-1800) and Shimadzu UV-Visible-NIR Spectrometer (DMP-2800) respectively with $BaSO_4$ as a reference for solid state measurements. Field emission-scanning electron microscopy (FE-SEM) micrographs were recorded using a JEOL JSM-7100F instrument employing an 18 kV accelerating voltage. The zeta potential was recorded using a Zetasizer Nano ZS light-scattering apparatus (Malvern Instruments, U.K.). Optimization of Biginelli reaction was monitored by gas chromatography using dodecane as an internal standard (Bruker 450-GC; equipped with a capillary column HP-5, 30m × 0.25 mm; using a flame ionization detector).

Synthesis of $\{[Zn_2(5NO_2\text{-}IP)_2(L)_2](H_2O)\}_n$ (ADES-1): In a typical procedure, 3 mL H_2O:MeOH (1:1/v:v) solution was used to dissolve 5-nitroisophthalic acid (**$5NO_2\text{-}H_2IP$**) (21.1 mg, 0.1 mmol), KOH (11.2 mg, 0.2 mmol) and (E)-N'-(pyridin-3-ylmethylene)nicotinohydrazide (**L**) (22.6 mg, 0.1 mmol). Separately, 3 mL H_2O was added to $Zn(ClO_4)_2{\cdot}6H_2O$ (37.2 mg, 0.1 mmol) to prepare a metal solution. In a narrow test tube, ligand solution was carefully layered over metal solution with 8 mL buffer solution of H_2O:MeOH (1:1/v:v). The test tube was sealed and left for slow diffusion of precursors at room temperature, to afford quality colorless crystals within 10 days. (yield ~78%). Anal. Calcd. for $\{[Zn_2(\mathbf{5NO_2\text{-}IP})_2(\mathbf{L})_2](H_2O)\}_n$ (ADES-**1**): C, 46.30; H, 2.89; N, 13.49.%; Found: C, 45.98; H, 3.02; N, 13.19.%. FTIR (cm^{-1}, KBr): 3410 (br), 3215 (br), 3091 (s), 1705 (s),

1627 (s), 1567 (s), 1534 (s) 1457 (s), 1359 (s), 1292 (s), 1154 (m), 1029 (m), 924 (w), 861 (w), 830 (w), 736 (s), 629 (w), 528 (w).

Synthesis of $\{[Cd_2(5NO_2\text{-}IP)_2(L)_2](H_2O)_4(L)(CH_3OH)\}_n$ (ADES-2): The same method as for ADES-**1** was adopted with 3 mL aqueous solution of $Cd(ClO_4)_2{\cdot}xH_2O$ (31.1 mg, 0.1 mmol) in place of $Zn(ClO_4)_2{\cdot}6H_2O$. The narrow test tube was covered and allowed to stand for crystallization at ambient temperature, to afford quality pale yellow crystals within 10 days. (~74% yield). Anal. Calcd. for $\{[Cd_2(\mathbf{5NO_2\text{-}IP})_2(\mathbf{L})_2](H_2O)_4(\mathbf{L})\}_n$ (ADES-**2**): C, 44.68; H, 3.85; N, 12.58.%; Found: C, 43.98; H, 3.32; N, 12.09%. FTIR (cm^{-1}, KBr): 3417 (br), 3221 (br), 3092 (s), 1622 (s), 1563 (s), 1514 (s), 1449 (s), 1422 (s), 1362 (s), 1293 (s), 1196 (w), 1126 (m), 1082 (w), 923 (w), 854 (w), 790 (w), 736 (s), 626 (w), 526 (w).

Bulk synthesis of ADES-1 by conventional (reflux) method: Bulk powder of ADES-**1** was synthesized by heating a mixture of $Zn(NO_3)_2{\cdot}6H_2O$ (10 mmol), **$5NO_2\text{-}H_2IP$** (10 mmol), KOH (20 mmol), and **L** (10 mmol) in 150 mL of H_2O:MeOH (1:1/v:v) at 70 °C for 6h. The obtained precipitates were filtered and thoroughly washed with methanol/water (1/1) followed by acetone. The material was allowed to dry at ambient temperature (yield ~86%) which has been used for dye adsorption and catalytic studies.

Adsorption of the organic dyes by ADES-1: The adsorption experiment was performed with a 5 × 10^{-5} M aqueous solution of organic dyes viz. methyl violet (MV), methylene blue (MB), methyl orange (MO) and rhodamine B (RhB). The 100 mg MOF material (ADES-**1**) was added to the 10 mL solution of respective dye and stirred continuously for 3 h. After that, adsorbent was isolated via centrifuge to afford adsorbed dye solution. The concentration of resulting dye

solution was monitored by UV-Vis spectroscopy. The amount of dye adsorbed after 3 h, was calculated by following equation considering initial and equilibrium concentration of dyes solution.

$$q_e = (C_i - C_e)V \times MW/m \qquad \text{(Equation S1)}$$

Where, C_i-initial concentration of dyes (moles/L), C_e-equilibrium concentration of dyes (moles/L), V-volume of the solution (L), MW-molecular weight of dye and m-mass of the adsorbent (g).

The following equation was used to find dyes removal percentage (η):

$$\eta = (C_i - C_e)/C_i \times 100\% \qquad \text{(Equation S2)}$$

To investigate the adsorption capacity of ADES-**1** in mixture of dyes, 10 mL aqueous solution of MV+RhB, MB+RhB and MO+RhB (1:1, v/v) was stirred with 100 mg ADES-**1** for 3 h. The concentration of adsorbed dye solution was monitored by UV-Vis spectroscopy.

Dye separation through chromatographic column filled with ADES-1: In each individual separation 10^{-4} M aqueous solution of organic dyes MV, MB, MO and RhB were used. A 15 cm long and 0.5 cm wide chromatographic column was packed with aqueous slurry of ADES-**1** up to 5 cm and aqueous solutions of dyes were allowed to pass through the column at ambient temperature. To check the separation mixture of dyes, equal volume of MV+RhB, MB+RhB and MO+RhB were allowed to pass through the column under same condition. The concentrations of discharge solutions were investigated by UV-Vis spectra to determine the separation capability of ADES-**1**.

Dye desorption ability of ADES-1: To investigate the dye desorption ability of ADES-**1**, 20 mg dye-adsorbed materials ADES-**1**@MV, ADES-**1**@MB, ADES-**1**@MO and ADES-**1**@RhB were taken in a glass cuvette separately followed by addition of 1 mL MeOH. Individual cuvette was place in a spectrophotometer to record UV-Vis spectra at regular intervals over a total period of 90 min.

Procedure for Biginelli reaction: A mixture of aldehyde (1 mmol), ethyl acetoacetate (1 mmol) and urea (1.5 mmol) was reacted in a 10 mL flask at 80 °C in the presence of ADES-**1** (0.020 mmol). The reaction mass was heated for appropriate time as indicated by TLC. After completion of reaction, the reaction mixture was treated with cold water to remove any unreacted starting materials. After that, ethanol was added to the solid mass to separate the catalyst through centrifuge. Separated catalyst was washed with methanol/water (1/1) followed by acetone and successfully reused in the subsequent reactions. The crude products were purified by crystallization and the formation of desired products was confirmed by ^{1}H NMR and ^{13}C NMR data.

X-ray Crystallography: For both MOFs (ADES-**1** and ADES-**2**) crystals suitable for X-ray crystallography were obtained by layering of the metal salts and ligand precursors mentioned in the experimental section. The crystal data were collected on a Bruker D8 Quest diffractometer, with CMOS detector in shutter less mode. The crystals were cooled to 150 K using an Oxford Cryostream liquid nitrogen cryostat. The instrument was equipped with a graphite monochromatized MoK_α X-ray source (λ = 0.71073 Å), with Triumph™ X-ray source optics. Data collection and initial indexing and cell refinement were handled using APEX II software.[S2] Frame integration, including Lorentz-polarization

corrections, and final cell parameter calculations were carried out using SAINT+ software.[S3] The data were corrected for absorption using the SADABS program.[S4] Decay of reflection intensity was monitored by analysis of redundant frames. The structure was solved using Direct methods and difference Fourier techniques. Non-hydrogen atoms were refined anisotropically, structure solution and refinement were performed with SHELXTL.[S5] In the case of ADES-**2**, hydrogens attached to the lattice water molecules could not be located from the difference Fourier map. After the complete convergence of the MOF network along with **L** and one water molecule for ADES-**2**, a series of scattered peaks having close proximity with residual electron density ranging from ~3.5 e $Å^{-3}$ to 2 e $Å^{-3}$ were observed in the difference Fourier map corresponding to highly disordered solvent molecule present in the crystal lattice. Since the residual electron density was weak and there were no obvious major site occupations for the lattice solvent molecules. Attempts to model these disordered peaks were unsuccessful. PLATON/SQUEEZE was used to mask the contribution from the disordered lattice solvent molecule (methanol and water).[S6] The solvent accessible void volume and the corresponding electron counts/unit cell estimated was 369 $Å^3$/110 $eÅ^{-3}$ for ADES-**2**. This electron count corresponds to approximately six disordered methanol molecules present in the unit cell as the solvent of crystallization for ADES-**2**. The final cycles of least-square refinements with the modified dataset after masking the contribution from the disordered solvent molecules significantly improved the R-values and goodness for ADES-**2**. CCDC numbers 2014940-2014941 corresponds to both the compounds reported

in this manuscript and this data can be obtained free of charge from The Cambridge Crystallographic Data Center via www.ccdc.cam.ac.uk/data_request/cif

Table S1. Crystal Data and Refinement Parameters for ADES-**1** and ADES-**2**.

Identification code	ADES-**1**	ADES-**2**
Chemical formula	$ZnC_{20}H_{15}N_5O_8$	$CdC_{26}H_{18}N_7O_{8.50}$
Formula weight (g/mol)	518.74	676.87
Crystal Color	Colorless	Pale Yellow
Crystal Size (mm)	0.08 x 0.11 x 0.12	0.09 x 0.14 x 0.21
Temperature (K)	150(2)	150(2)
Crystal System	Triclinic	Triclinic
Space Group	$P\bar{1}$	$P\bar{1}$
a(Å)	9.8794(12)	10.2194(10)
b(Å)	10.0399(12)	11.7451(12)
c(Å)	12.3173(15)	14.7018(15)
α(°)	105.888(4)	101.056(3)
β(°)	109.488(4)	95.464(3)
γ(°)	103.602(4)	111.560(3)
Z	2	2
V(Å^3)	1033.4(2)	1583.9(3)
Density (Mg/m^3)	1.667	1.419
μ(mm^{-1})	1.250	0.745
F(000)	528	678
Reflections Collected	38367	45142
Independent Reflections	6351	9724
R_{int}	0.0468	0.0392
Number of parameters	367	388
GOF on F^2	1.059	1.109
Final R_1/wR_2 ($I \geq 2\sigma(I)$)	0.0291/0.0652	0.0388/0.1343
Weighted R_1/wR_2 (all data)	0.0392/0.0701	0.0456/0.1403
CCDC number	2014941	2014940
$R = \Sigma\|\|F_o\| - \|F_c\|\|/\Sigma\|F_o\|$; $wR = [\Sigma w(F_o^2 - F_c^2)^2/\Sigma w(F_o^2)^2]^{1/2}$		

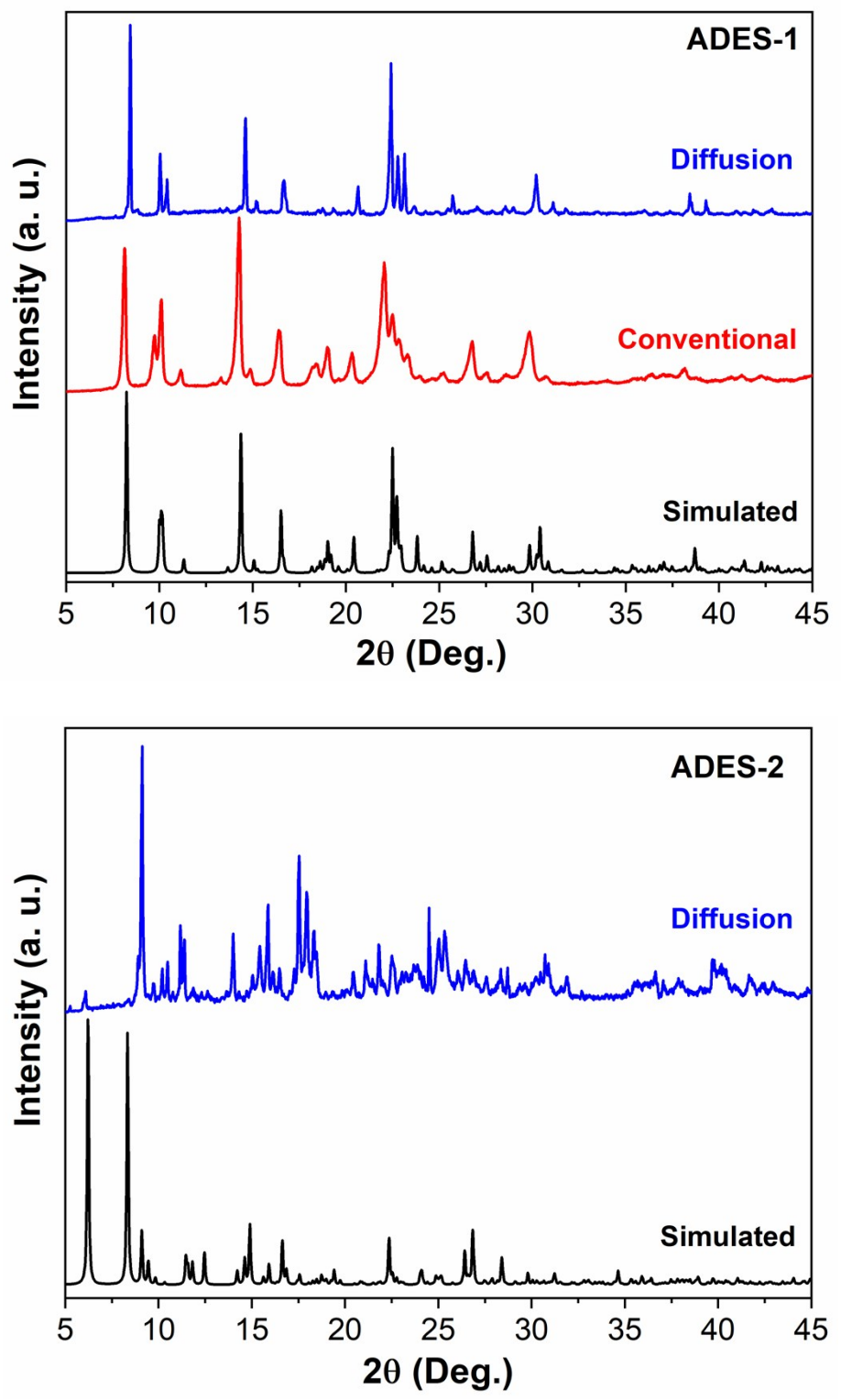

Figure S1. PXRD patterns of ADES-**1** (conventional and diffusion) and ADES-**2** (diffusion) confirmed by comparison with simulated pattern.

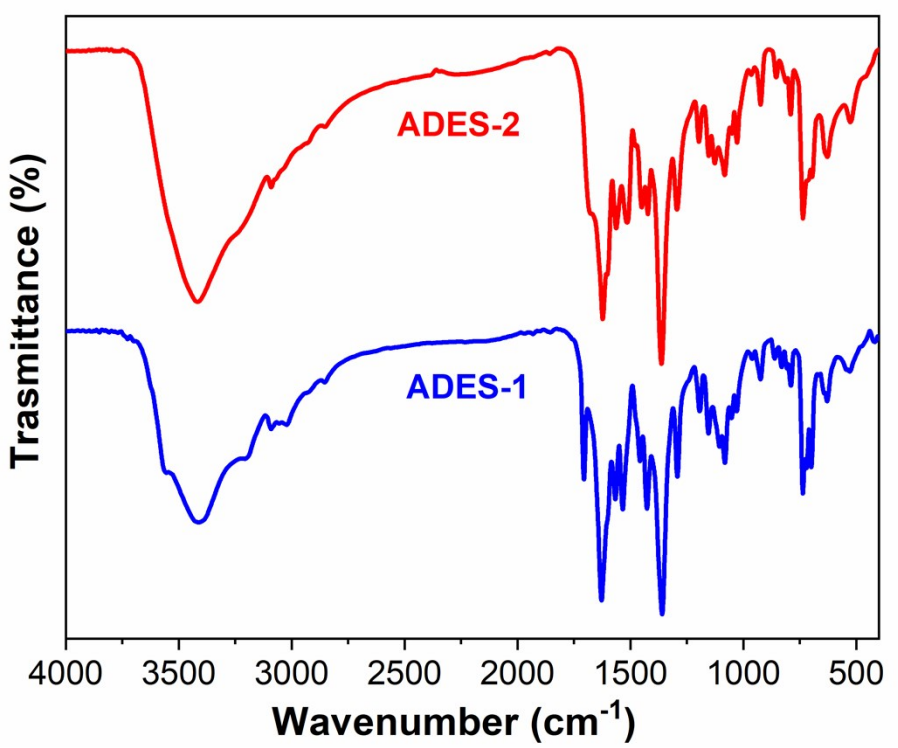

Figure S2. FTIR spectra of ADES-**1** and ADES-**2** recorded by dispersing in KBr pellet

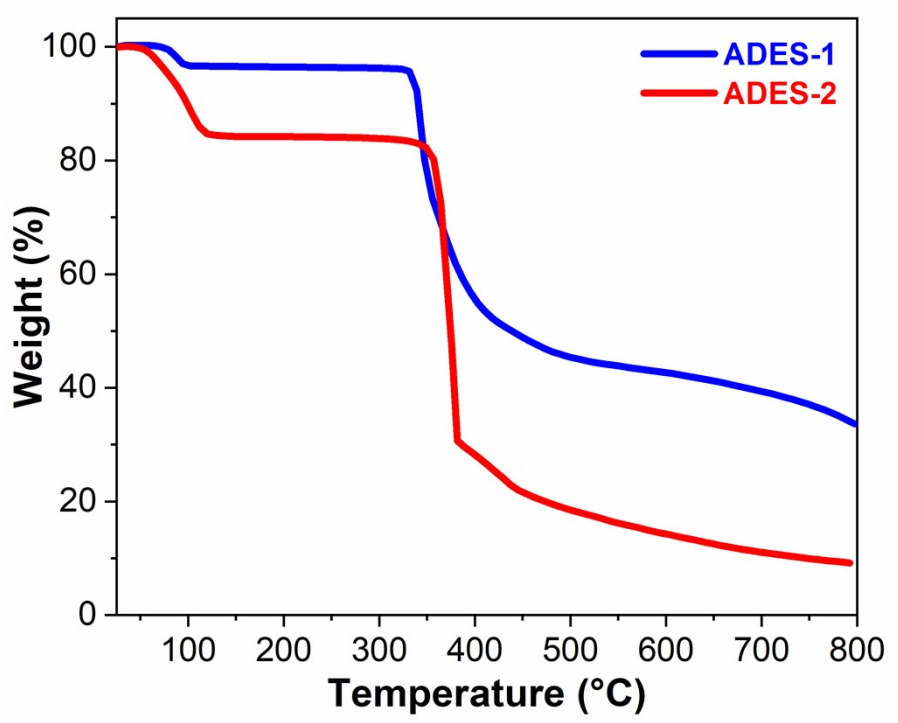

Figure S3. TG analysis of compound ADES-**1** and ADES-**2** in N_2 atmosphere.

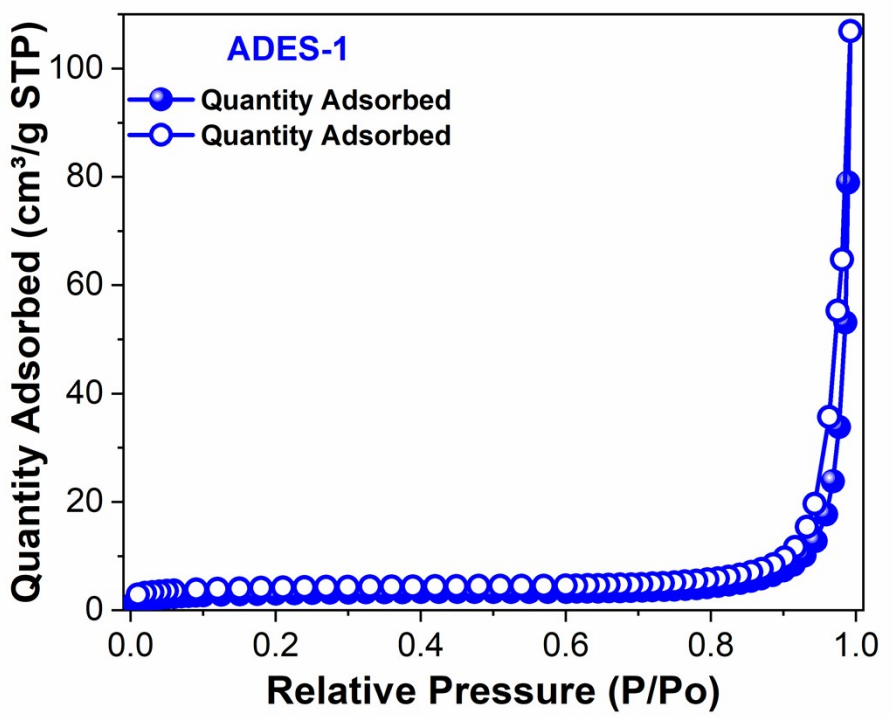

Figure S4. N_2 adsorption isotherm of ADES-**1** at 77 K.

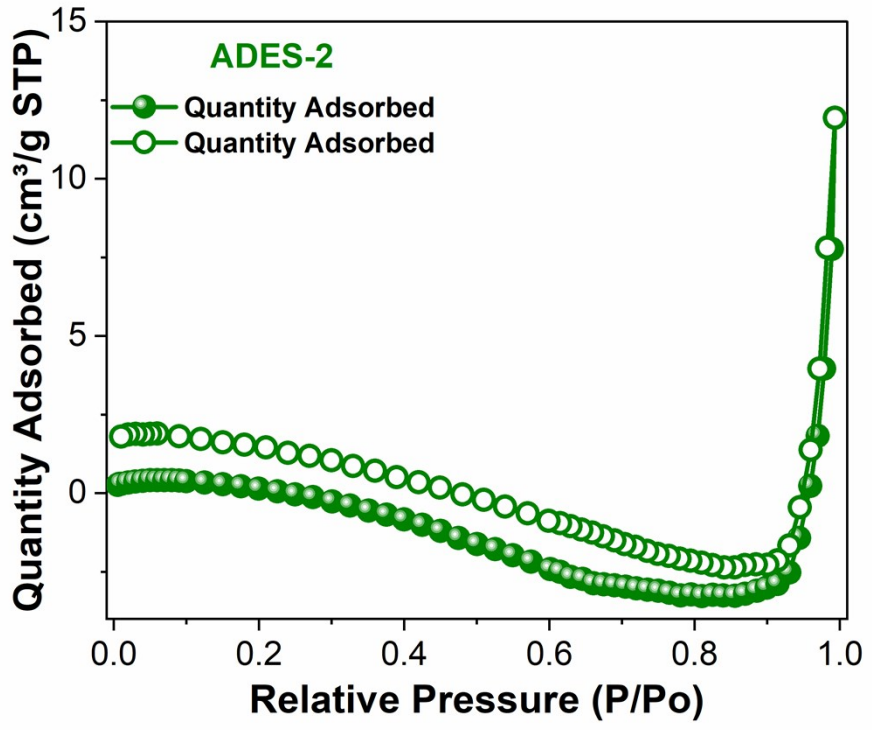

Figure S5. N_2 adsorption isotherm of ADES-**2** at 77 K.

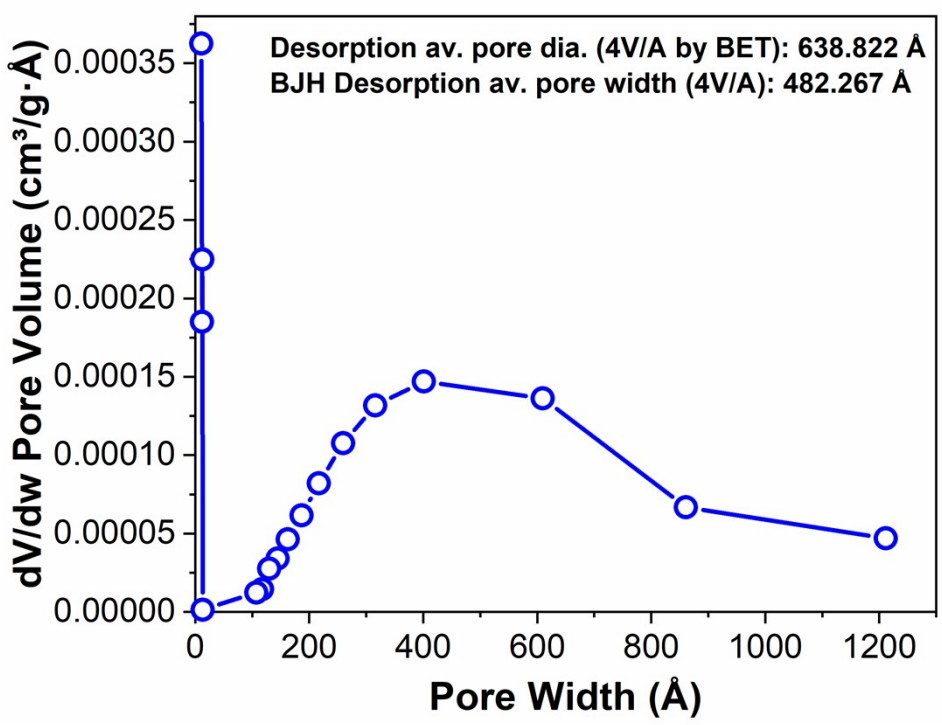

Figure S6. BJH Desorption dV/dD Pore Volume plot for ADES-**1**.

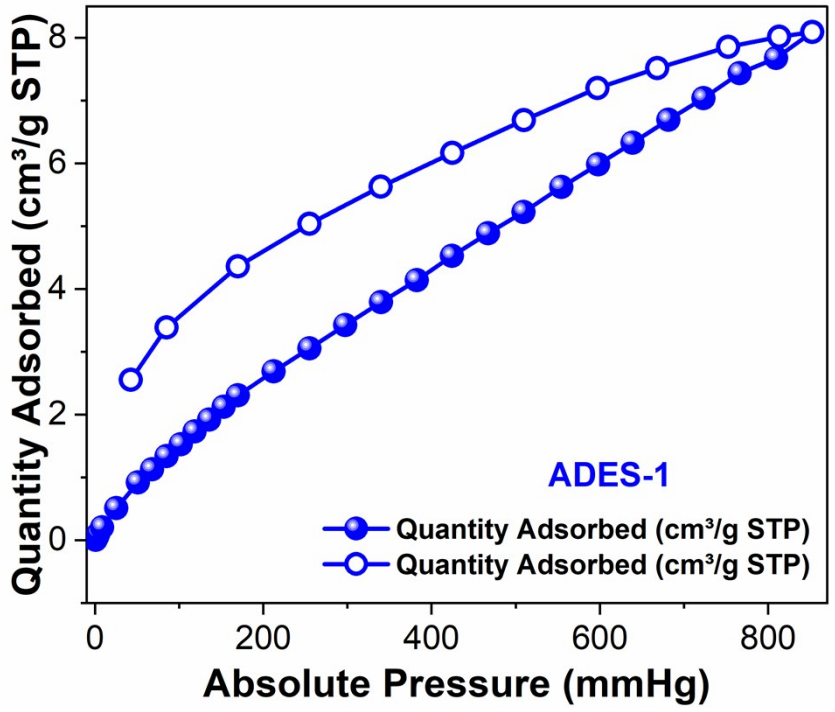

Figure S7. CO_2 adsorption isotherm of ADES-**1** at 273 K.

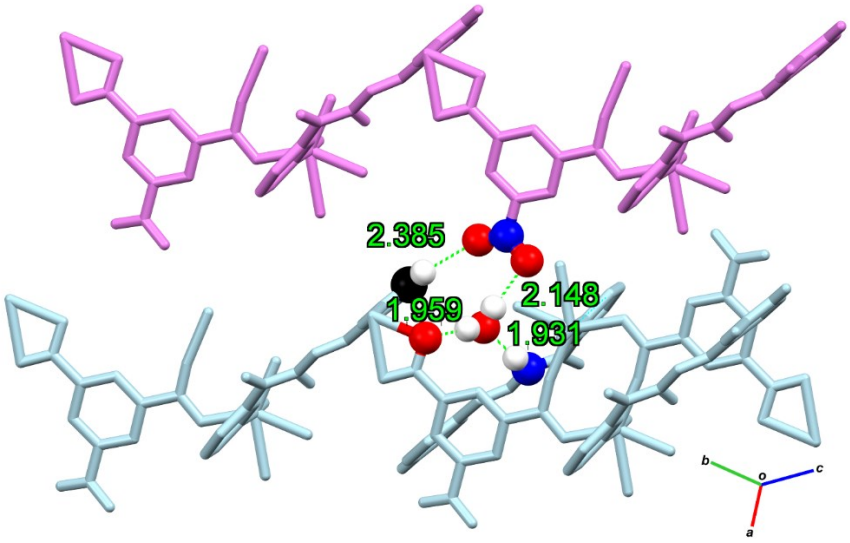

Figure S8. Hydrogen bonding interactions observed in ADES-**1**.

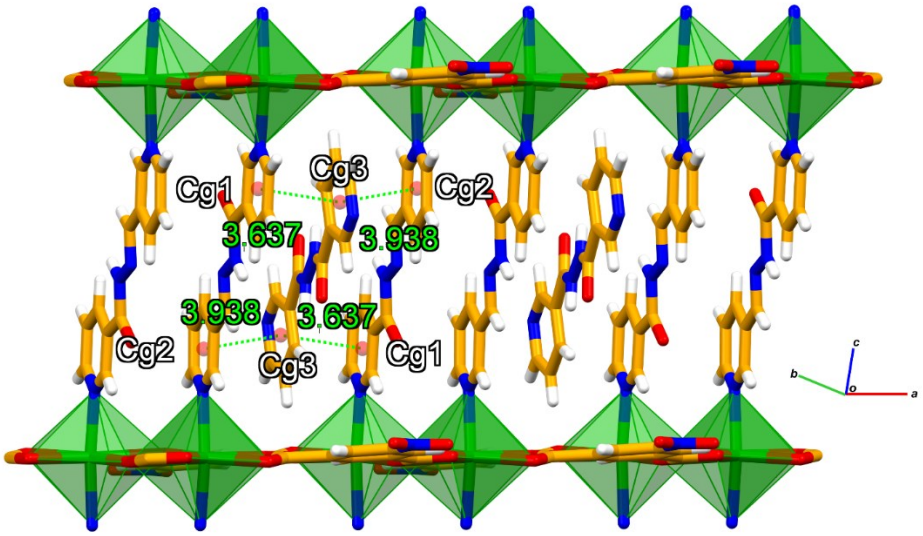

Figure S9. π···π stacking interactions observed in ADES-**2**.

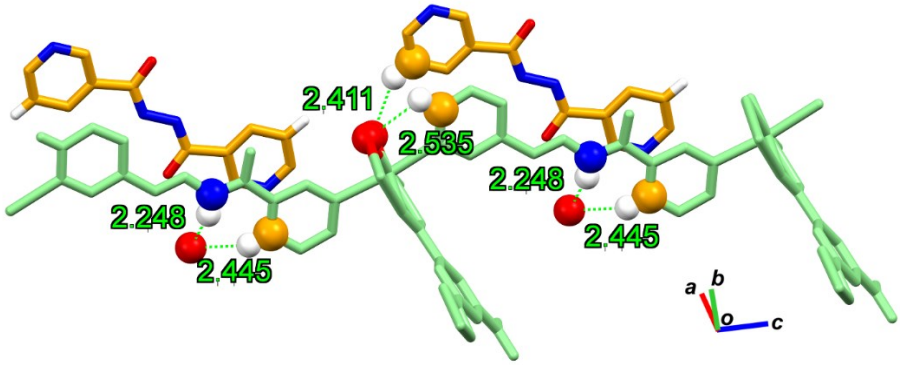

Figure S10. Hydrogen bonding interactions observed in ADES-**2**.

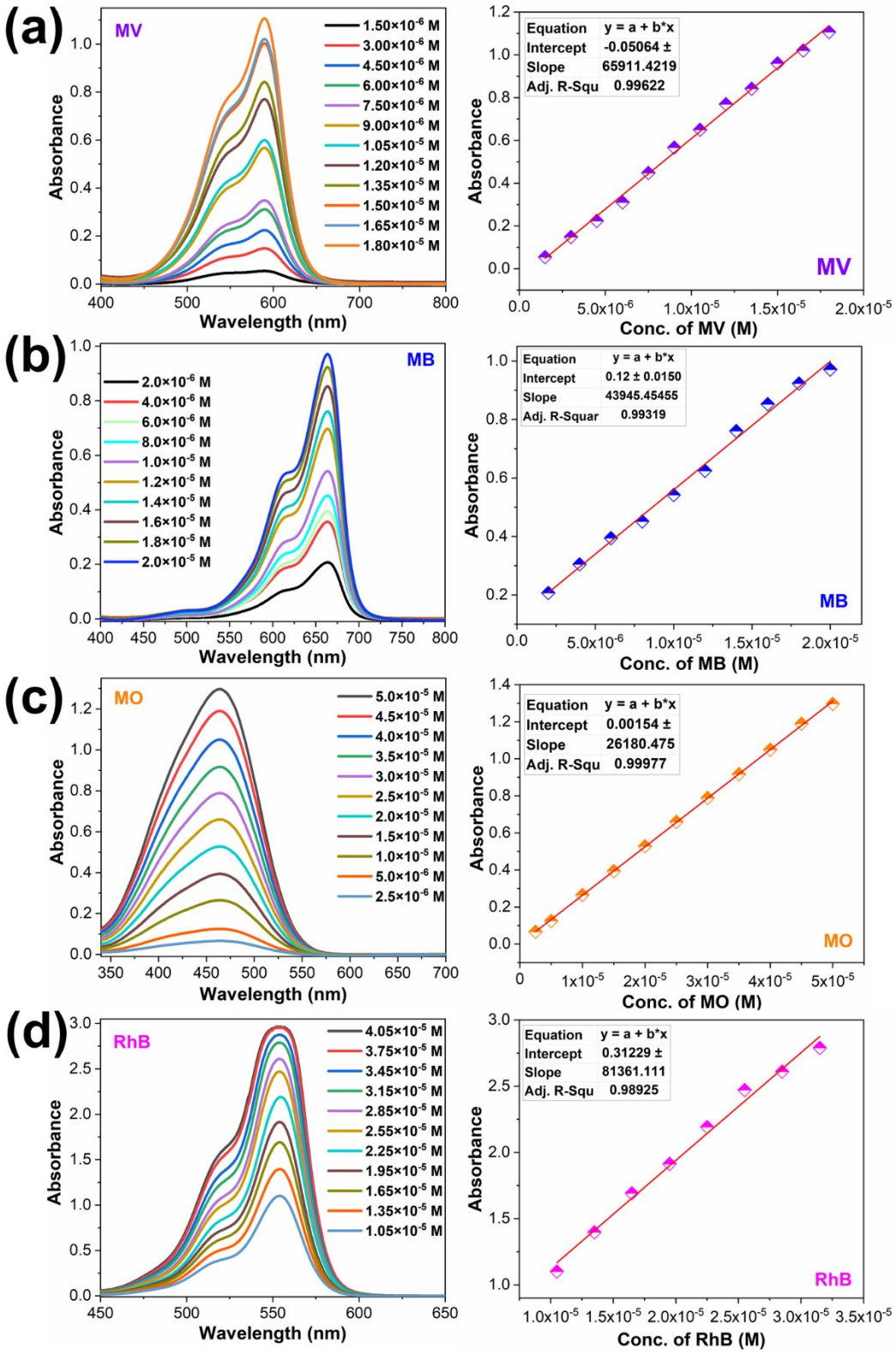

Figure S11. UV-Vis calibration and their Absorbance vs concentration plots of standard organic dyes MV, MB, MO and RhB (a, b, c and d).

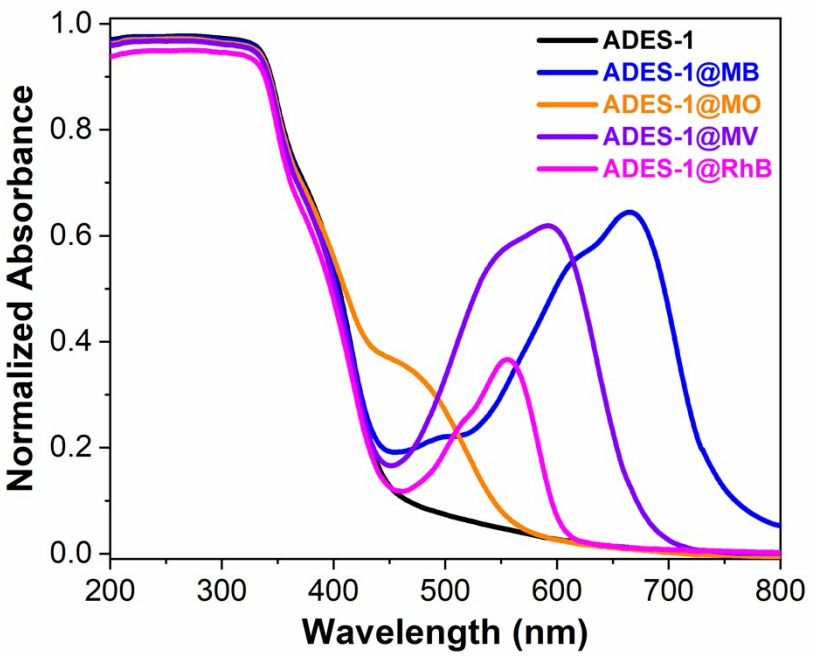

Figure S12. Solid state UV-Vis spectra of ADES-**1** and ADES-**1**@Dye materials confirming the adsorbents characteristic bands at particular wavelengths after adsorption of organic dyes.

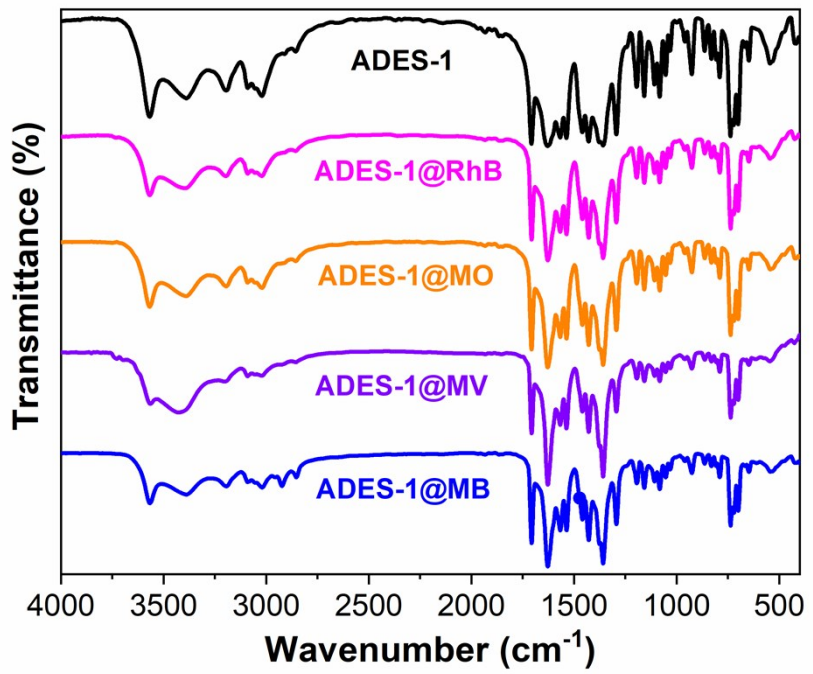

Figure S13. FTIR spectra of ADES-**1** and ADES-**1**@Dye corroborating the functionality of framework before and after adsorption of organic dyes.

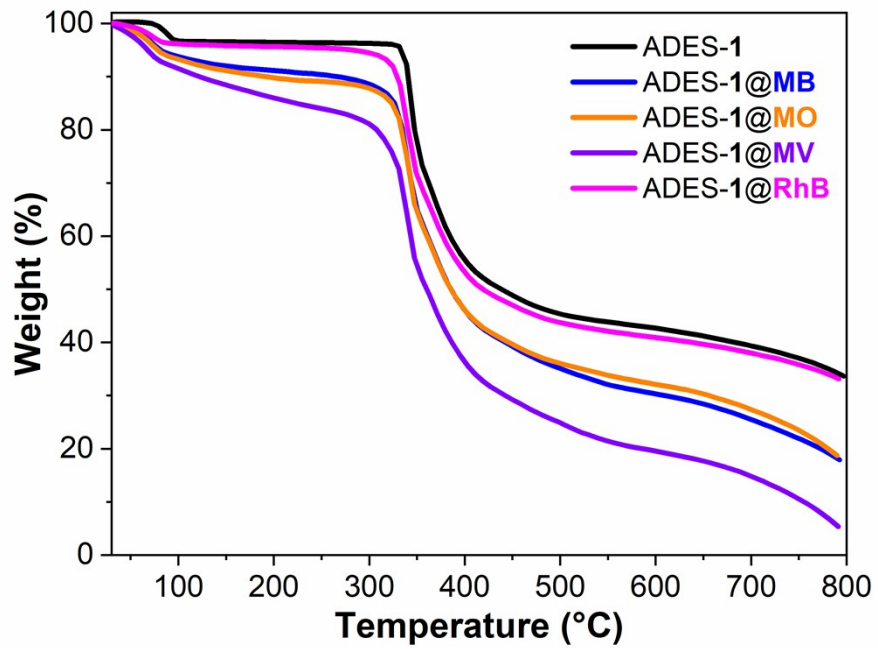

Figure S14. TG analysis of ADES-**1** and ADES-**1**@Dye confirming the thermal stability of ADES-**1** before and after absorption of organic dyes.

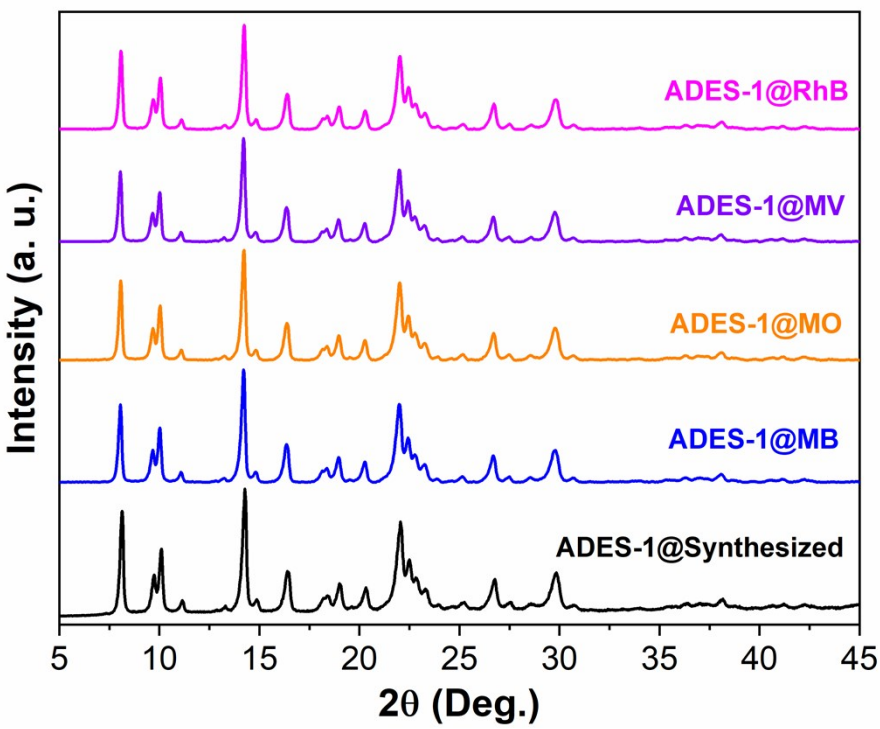

Figure S15. PXRD patterns of ADES-**1** and ADES-**1**@Dye confirming the stability of framework after adsorption of organic dyes.

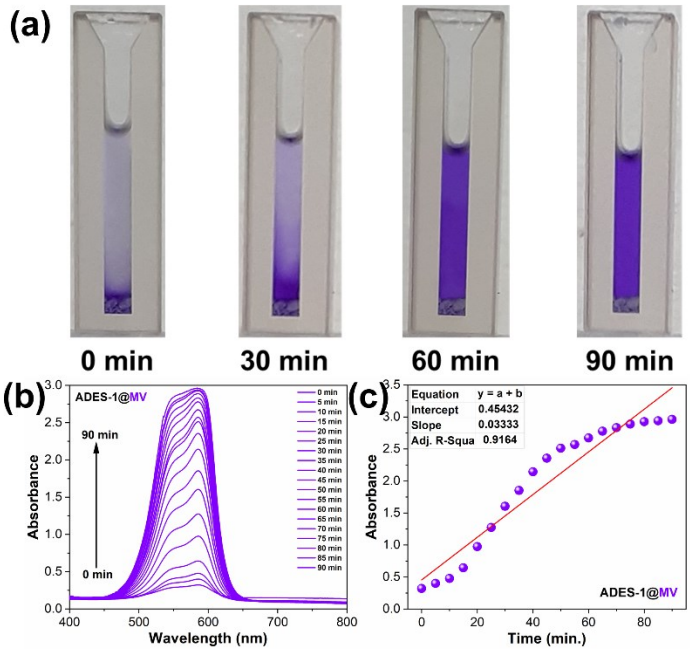

Figure S16. (a) Digital photographs demonstrating gradual colour change due to release of MV in 1 mL MeOH after soaking of 20 mg ADES-**1**@MV; (b) Time-dependent UV-Vis spectra representing the steady increase in the absorbance (λ_{max} = 587 nm) due to release of MV with time; (c) linear plot of absorbance vs time for the release of MV over a 90 min period.

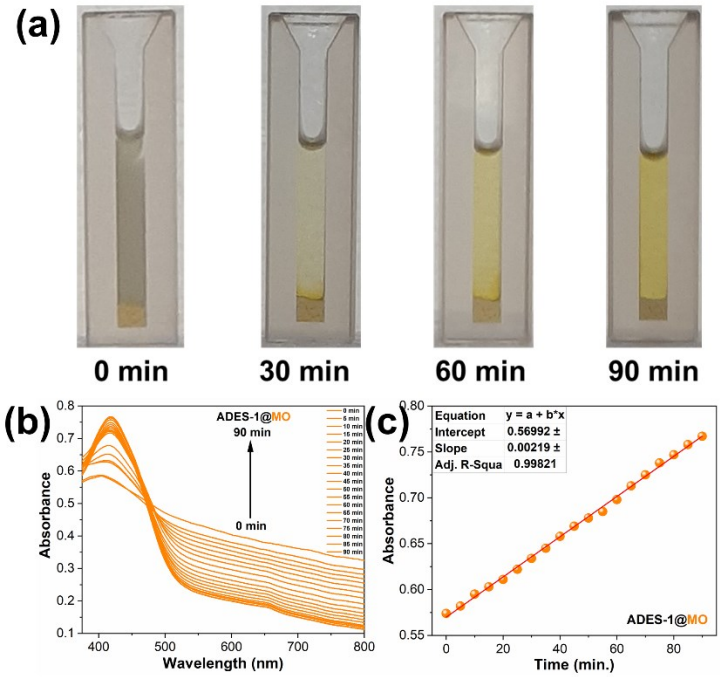

Figure S17. (a) Digital photographs demonstrating gradual colour change due to release of MO in 1 mL MeOH after soaking of 20 mg of ADES-**1**@MO; (b) Time-dependent UV-Vis spectra representing the steady increase in the absorbance (λ_{max} = 418 nm) due to release of MO with time; (c) linear plot of absorbance vs time for the release of MO over a 90 min period.

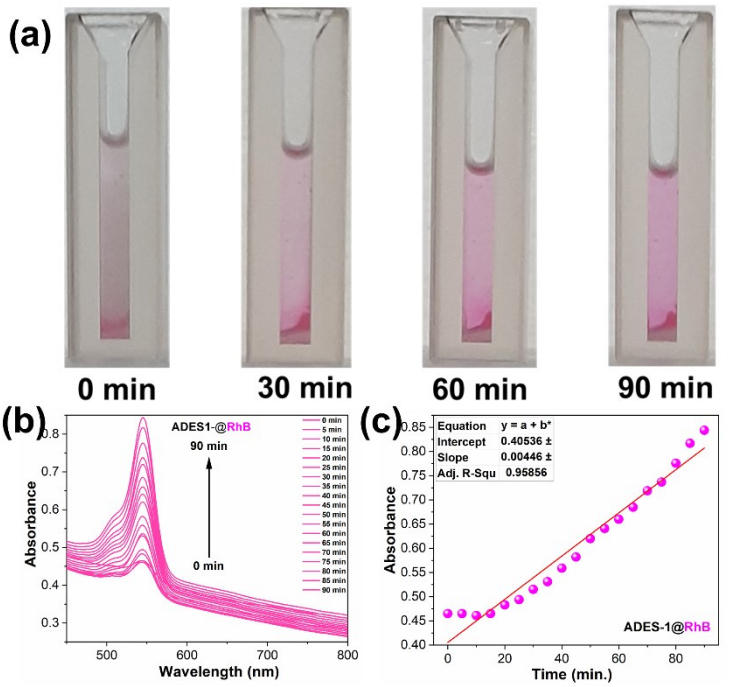

Figure S18. (a) Digital photographs demonstrating gradual colour change due to release of RhB in 1 mL MeOH after soaking of 20 mg of ADES-**1**@RhB; (b) Time-dependent UV-Vis spectra representing the steady increase in the absorbance (λ_{max} = 546 nm) due to release of RhB with time; (c) linear plot of absorbance vs time for the release of RhB over a 90 min period.

^{1}H & ^{13}C NMR analysis of dihydropyrimidinone products

^{1}H and ^{13}C NMR spectra of dihydropyrimidinone products involve in this study are matched well with reported in the literature.[S7-S9] ^{1}H and ^{13}C NMR data are as follows.

	**Ethyl 6-methyl-2-oxo-4-phenyl-1,2,3,4-tetrahydropyrimidine-5-carboxylate:** ^{1}H NMR (500 MHz, DMSO-d_6) δ 9.21 (s, 1H), 7.76 (s, 1H), 7.36 – 7.24 (m, 5H), 5.16 (d, *J* = 3.4 Hz, 1H), 4.00 (q, *J* = 7.1 Hz, 2H), 2.27 (s, 3H), 1.11 (t, *J* = 7.1 Hz, 3H). ^{13}C NMR (126 MHz, $CDCl_3$) δ 164.86, 151.65, 147.88, 144.38, 127.92, 126.79, 125.76, 98.77, 58.71, 53.47, 17.30, 13.60.
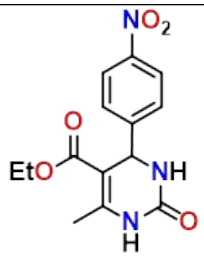	**Ethyl 6-methyl-4-(4-nitrophenyl)-2-oxo-1,2,3,4-tetrahydropyrimidine -5-carboxylate:** ^{1}H NMR (600 MHz, DMSO-d_6) δ 9.35 (s, 1H), 8.21 (d, *J* = 8.5 Hz, 2H), 7.89 (s, 1H), 7.50 (d, *J* = 9.2 Hz, 2H), 5.27 (d, *J* = 3.7 Hz, 1H), 3.97 (q, *J* = 7.3 Hz, 2H), 2.26 (s, 3H), 1.08 (t, *J* = 6.9 Hz, 3H). ^{13}C NMR (151 MHz, DMSO-d_6) δ 165.65, 152.53, 152.34, 149.96, 147.27, 128.23, 124.41, 98.76, 60.00, 54.22,

	18.41, 14.59.
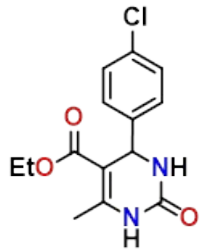	**Ethyl 4-(4-chlorophenyl)-6-methyl-2-oxo-1,2,3,4-tetrahydropyrimidine -5-carboxylate:** ^{1}H NMR (600 MHz, DMSO-d_6) δ 9.24 (s, 1H), 7.78 (s, 1H), 7.39 (d, *J* = 8.0 Hz, 2H), 7.24 (d, *J* = 7.9 Hz, 2H), 5.13 (d, *J* = 3.4 Hz, 1H), 3.97 (q, *J* = 7.1 Hz, 2H), 2.24 (s, 3H), 1.08 (t, *J* = 7.3 Hz, 3H). ^{13}C NMR (151 MHz, DMSO-d_6) δ 164.95, 151.67, 148.45, 143.47, 131.52, 128.13, 127.91, 98.56, 59.02, 53.11, 17.50, 13.77.
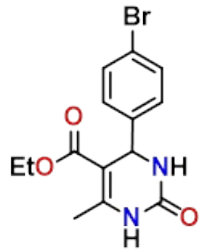	**Ethyl 4-(4-bromophenyl)-6-methyl-2-oxo-1,2,3,4-tetrahydropyrimidine -5-carboxylate:** ^{1}H NMR (600 MHz, DMSO-d_6) δ 9.25 (s, 1H), 7.78 (s, 1H), 7.52 (d, *J* = 8.0 Hz, 2H), 7.19 (d, *J* = 7.6 Hz, 2H), 5.13 (d, *J* = 4.2 Hz, 1H), 3.98 (q, *J* = 7.2 Hz, 2H), 2.25 (s, 3H), 1.09 (t, *J* = 7.3 Hz, 3H). ^{13}C NMR (151 MHz, DMSO-d_6) δ 164.99, 151.74, 148.52, 143.97, 131.11, 128.35, 120.11, 98.56, 59.07, 53.27, 17.59, 13.85.
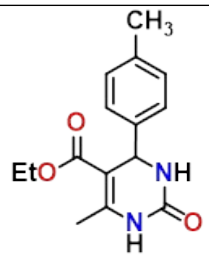	**Ethyl 6-methyl-2-oxo-4-(p-tolyl)-1,2,3,4-tetrahydropyrimidine-5-carboxylat**: ^{1}H NMR (600 MHz, DMSO-d_6) δ 9.16 (s, 1H), 7.69 (s, 1H), 7.11 (s, 4H), 5.10 (s, 1H), 3.97 (q, *J* = 6.9 Hz, 2H), 2.24 (d, *J* = 12.6 Hz, 6H), 1.10 (t, *J* = 7.0 Hz, 3H). ^{13}C NMR (151 MHz, DMSO-d_6) δ 165.01, 151.83, 147.79, 141.58, 136.03, 128.54, 125.78, 99.06, 58.82, 53.25, 20.28, 17.39, 13.73.
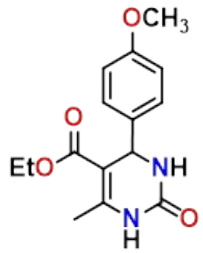	**Ethyl 4-(4-methoxyphenyl)-6-methyl-2-oxo-1,2,3,4-tetrahydropyrimidine -5-carboxylate:** ^{1}H NMR (600 MHz, DMSO-d_6) δ 9.15 (s, 1H), 7.67 (s, 1H), 7.14 (d, *J* = 8.6 Hz, 2H), 6.87 (d, *J* = 8.1 Hz, 2H), 5.09 (d, *J* = 3.7 Hz, 1H), 3.97 (q, *J* = 7.2 Hz, 2H), 3.71 (s, 3H), 2.23 (s, 3H), 1.10 (t, *J* = 6.9 Hz, 3H). ^{13}C NMR (151 MHz, DMSO-d_6) δ 165.28, 158.34, 152.06, 147.92, 136.95, 127.29, 113.60, 99.46, 59.06, 54.95, 53.22, 17.65, 14.00.
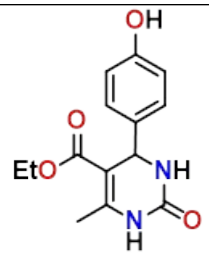	**Ethyl 4-(4-hydroxyphenyl)-6-methyl-2-oxo-1,2,3,4-tetrahydropyrimidine -5-carboxylate:** ^{1}H NMR (600 MHz, DMSO-d_6) δ 9.13 (s, 1H), 7.63 (s, 1H), 7.02 (d, *J* = 8.0 Hz, 2H), 6.69 (d, *J* = 7.8 Hz, 2H), 5.04 (s, 1H), 3.97 (q, *J* = 7.1 Hz, 2H), 2.23 (s, 3H), 1.10 (d, *J* = 7.6 Hz, 3H). ^{13}C NMR (151 MHz, DMSO-d_6) δ 165.39, 156.65, 152.19, 147.67, 135.24, 127.33, 114.96, 99.72, 59.06, 53.39, 17.67, 14.03.

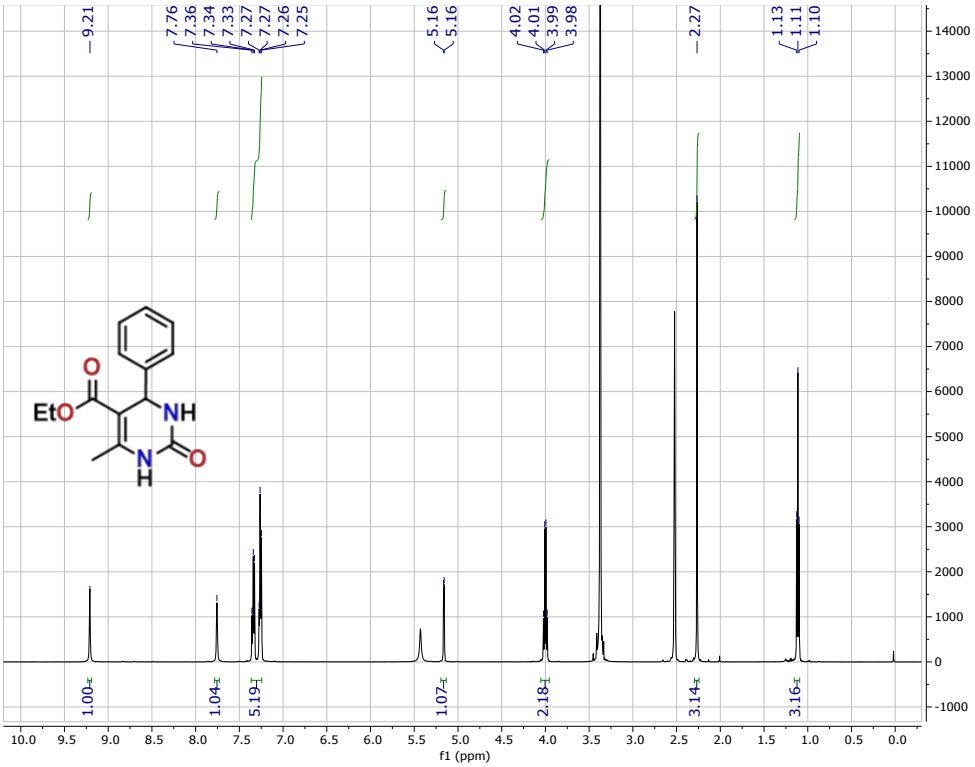

Figure S19. ^{1}H-NMR of the isolated ethyl 6-methyl-2-oxo-4-phenyl-1,2,3,4-tetrahydropyrimidine-5-carboxylate.

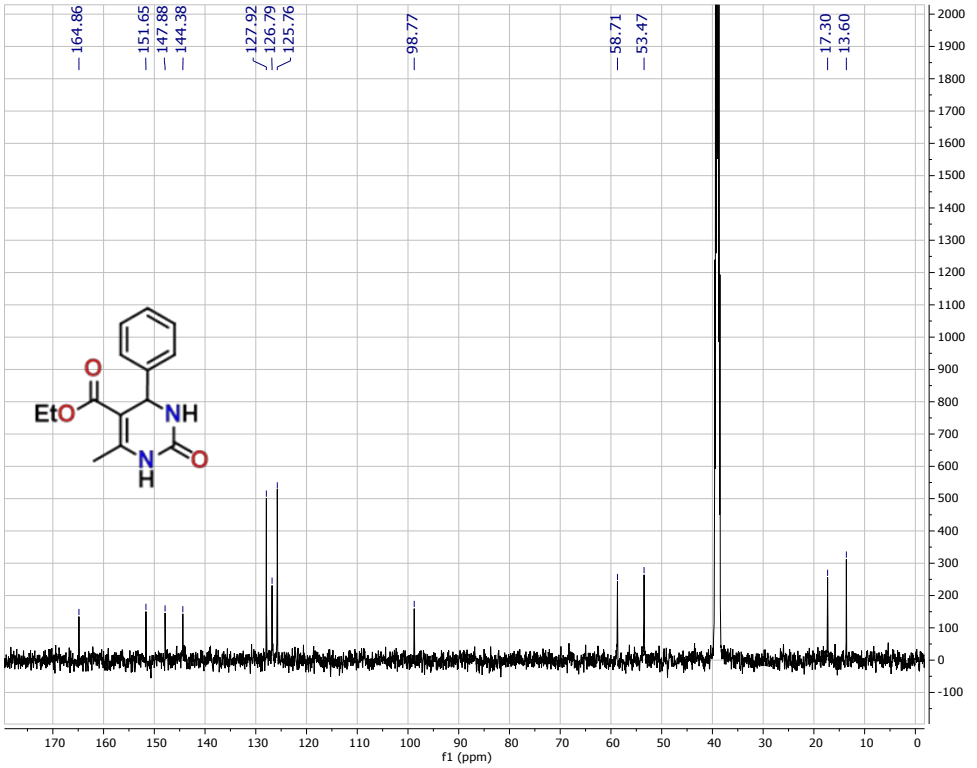

Figure S20. ^{13}C-NMR of the isolated ethyl 6-methyl-2-oxo-4-phenyl-1,2,3,4-tetrahydropyrimidine-5-carboxylate.

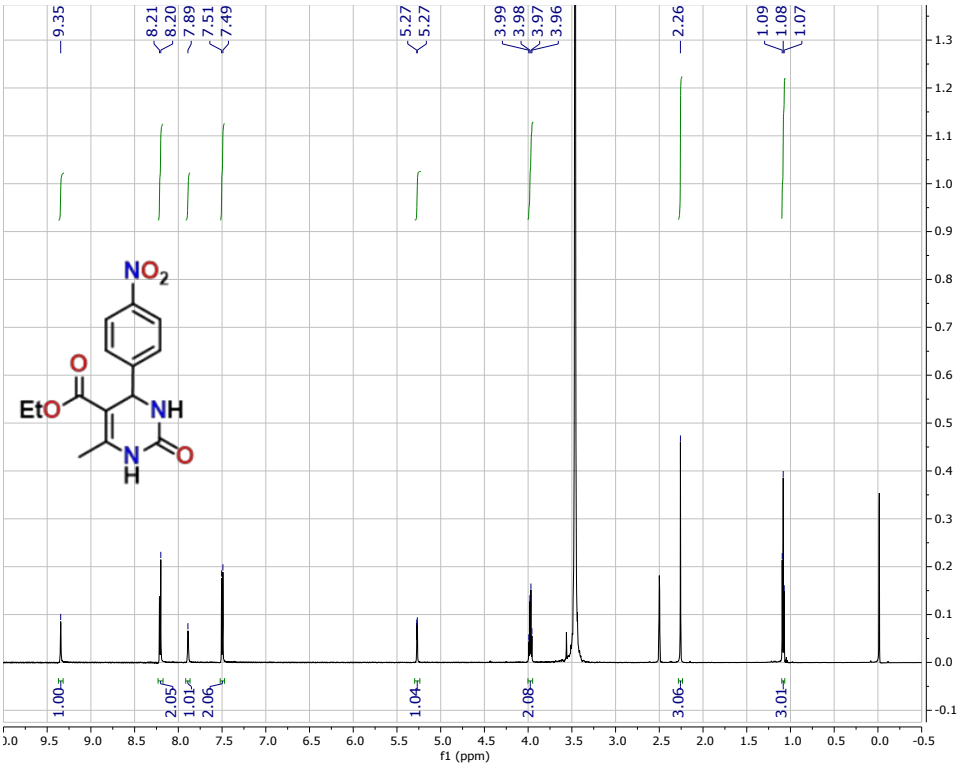

Figure S21. ^{1}H-NMR of the isolated ethyl 6-methyl-4-(4-nitrophenyl)-2-oxo-1,2,3,4-tetrahydropyrimidine-5-carboxylate.

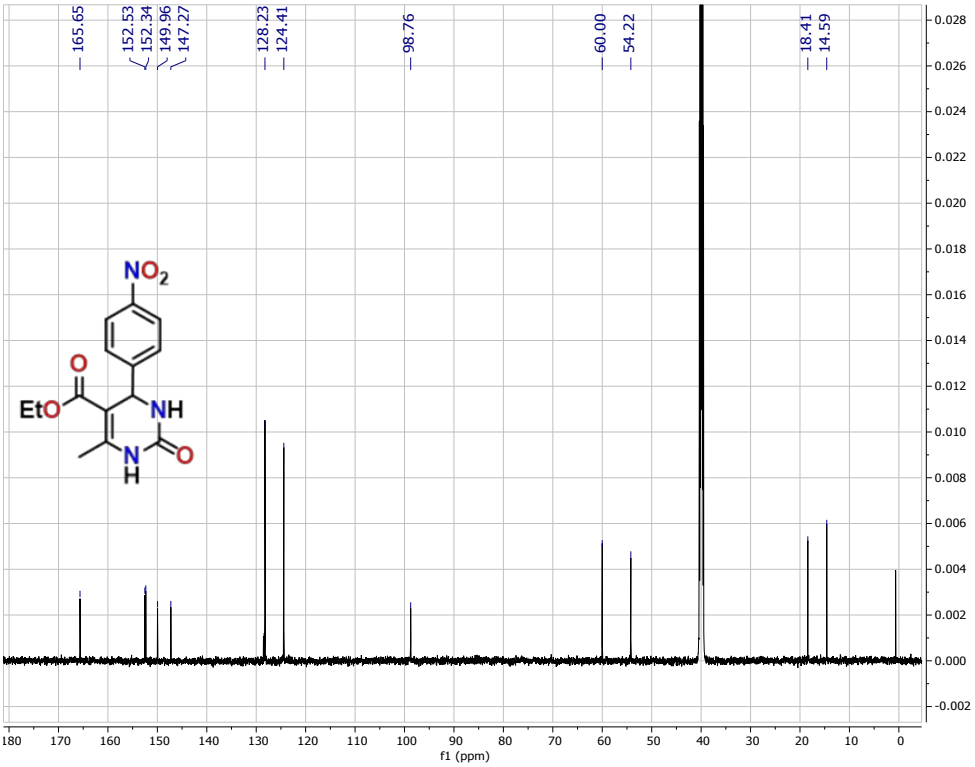

Figure S22. ^{13}C-NMR of the isolated ethyl 6-methyl-4-(4-nitrophenyl)-2-oxo-1,2,3,4-tetrahydropyrimidine-5-carboxylate.

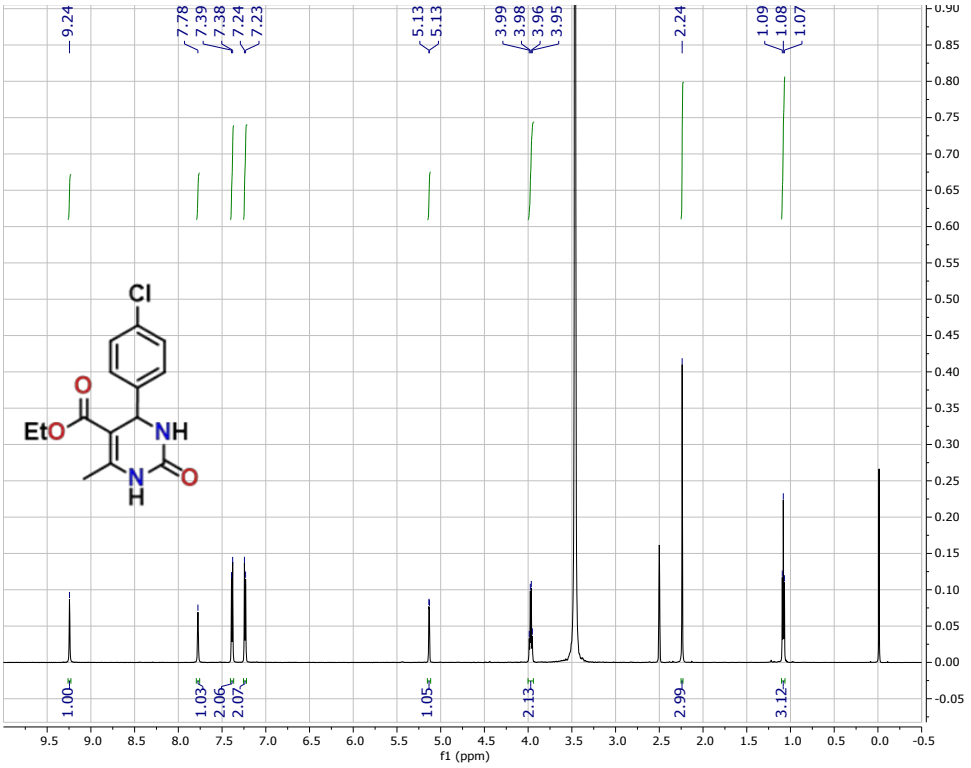

Figure S23. ^{1}H-NMR of the isolated ethyl 4-(4-chlorophenyl)-6-methyl-2-oxo-1,2,3,4-tetrahydropyrimidine-5-carboxylate.

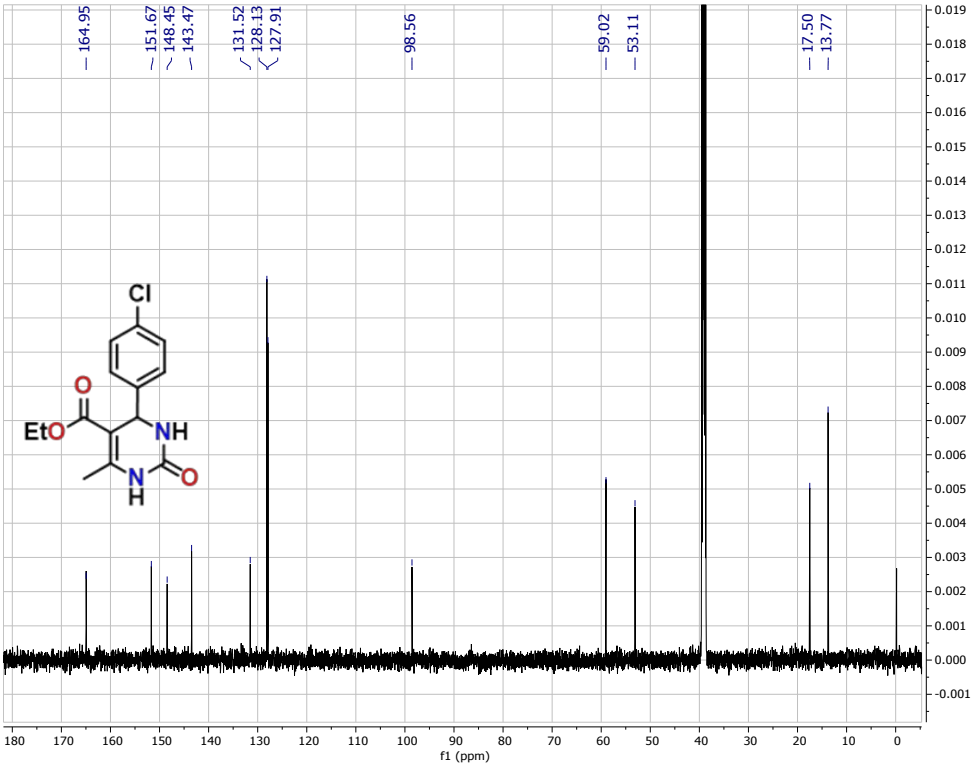

Figure S24. ^{13}C-NMR of the isolated ethyl 4-(4-chlorophenyl)-6-methyl-2-oxo-1,2,3,4-tetrahydropyrimidine-5-carboxylate.

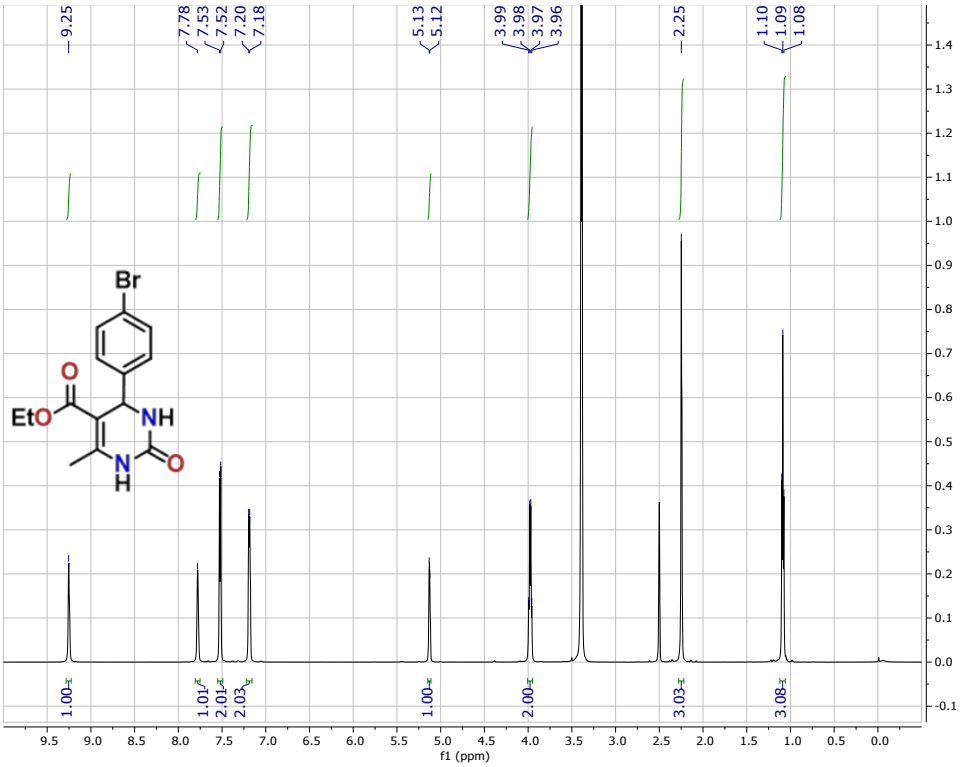

Figure S25. ^{1}H-NMR of the isolated ethyl 4-(4-bromophenyl)-6-methyl-2-oxo-1,2,3,4-tetrahydropyrimidine-5-carboxylate.

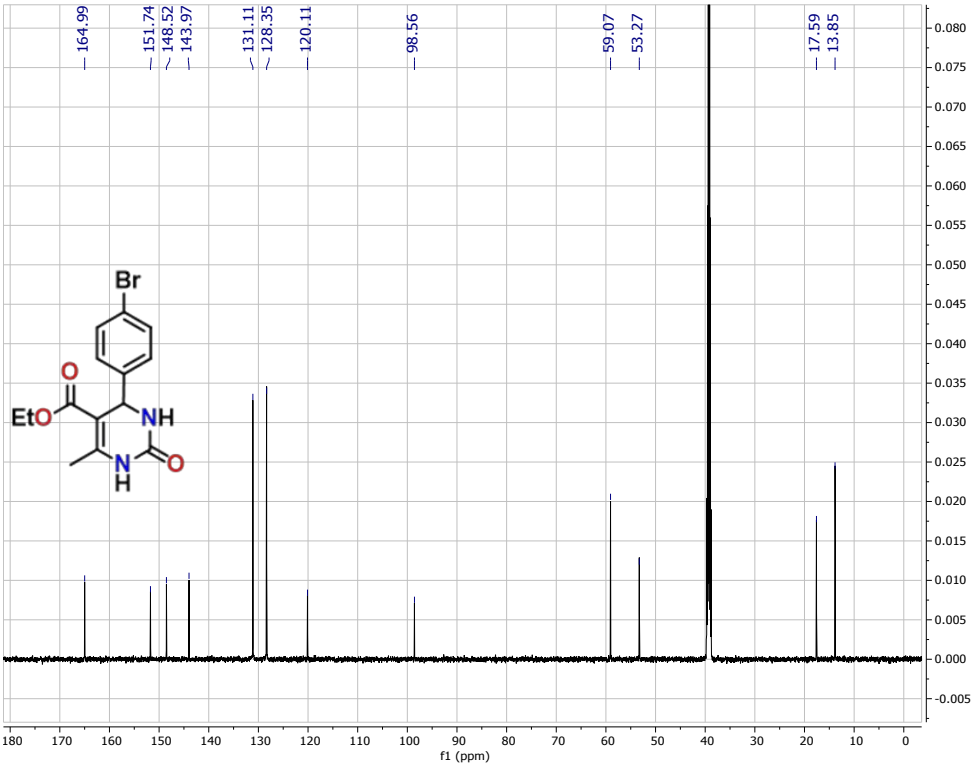

Figure S26. ^{13}C-NMR of the isolated ethyl 4-(4-bromophenyl)-6-methyl-2-oxo-1,2,3,4-tetrahydropyrimidine-5-carboxylate.

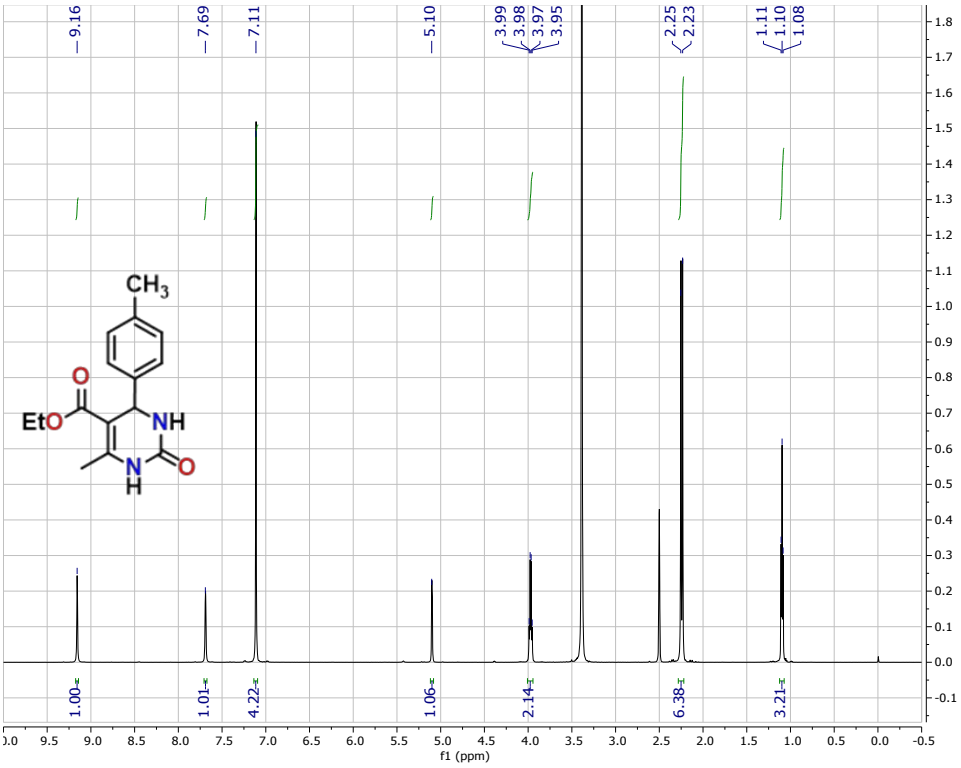

Figure S27. ^{1}H-NMR of the isolated ethyl 6-methyl-2-oxo-4-(p-tolyl)-1,2,3,4-tetrahydropyrimidine-5-carboxylate.

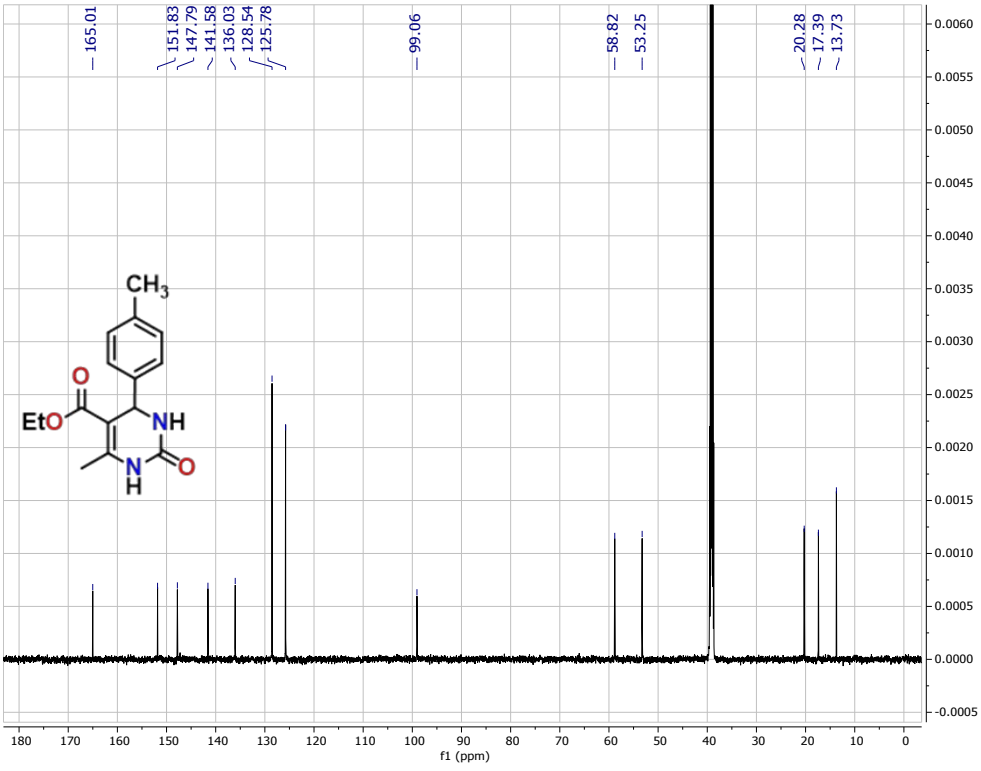

Figure S28. ^{13}C-NMR of the isolated ethyl 6-methyl-2-oxo-4-(p-tolyl)-1,2,3,4-tetrahydropyrimidine-5-carboxylate.

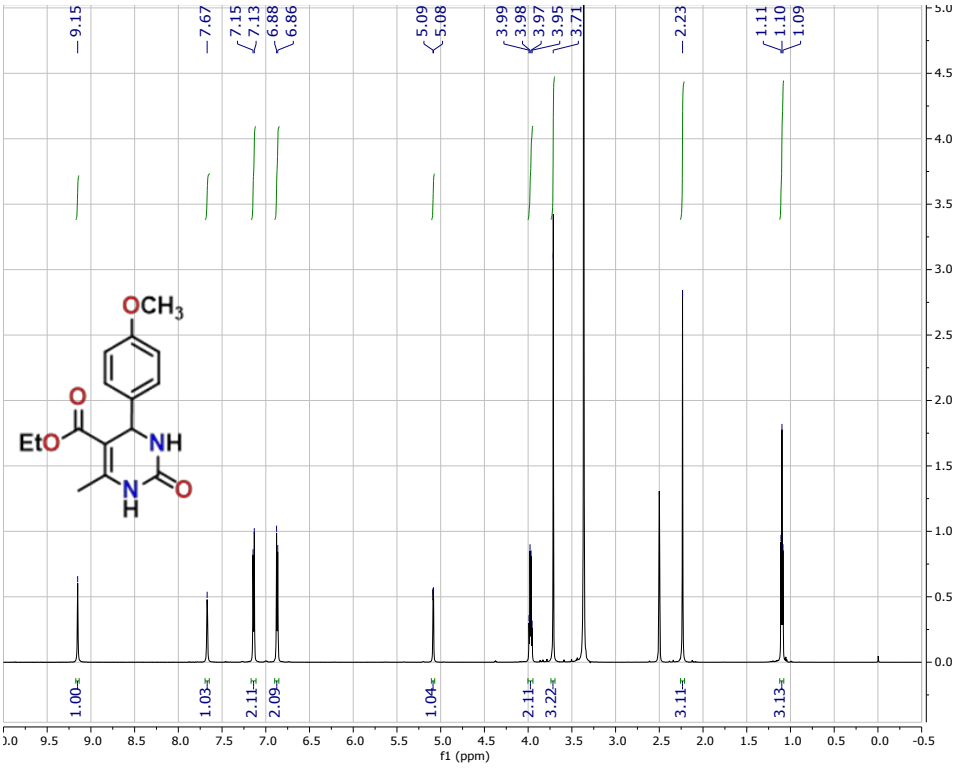

Figure S29. ^{1}H-NMR of the isolated ethyl 4-(4-methoxyphenyl)-6-methyl-2-oxo-1,2,3,4-tetrahydropyrimidine-5-carboxylate.

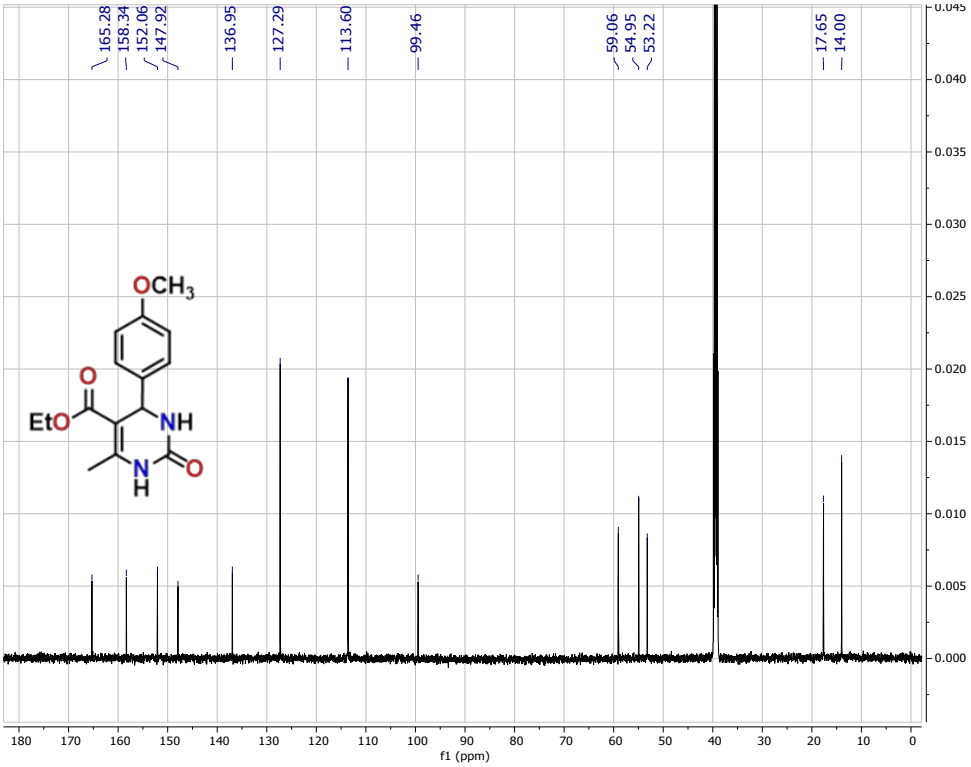

Figure S30. ^{13}C-NMR of the isolated ethyl 4-(4-methoxyphenyl)-6-methyl-2-oxo-1,2,3,4-tetrahydropyrimidine-5-carboxylate.

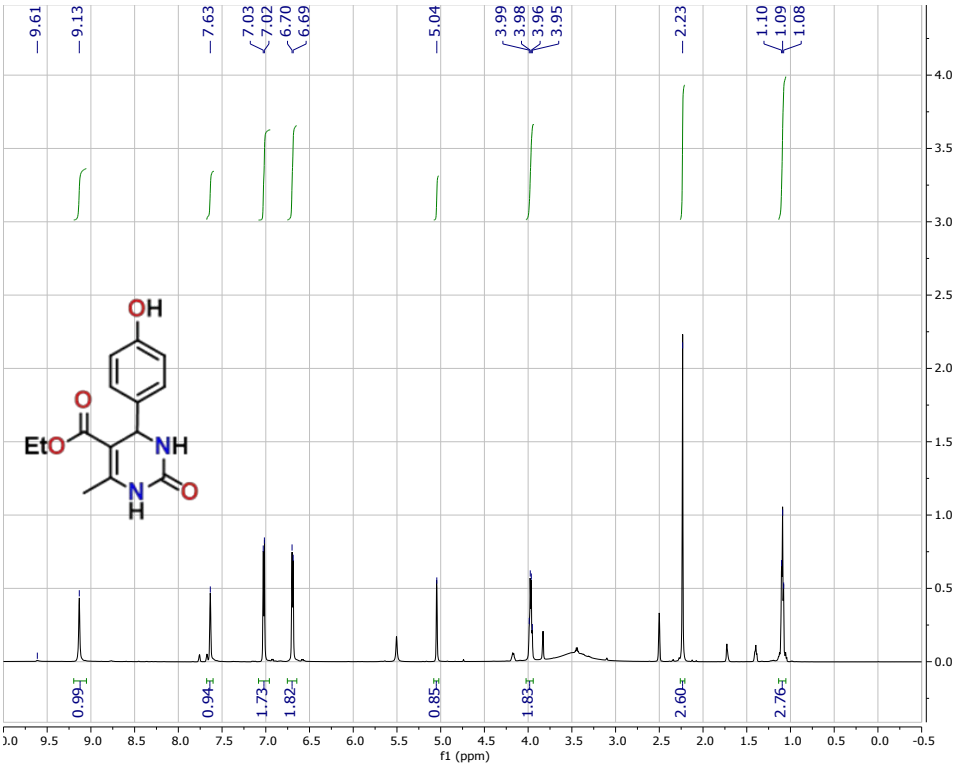

Figure S31. ^{1}H-NMR of the isolated ethyl 4-(4-hydroxyphenyl)-6-methyl-2-oxo-1,2,3,4-tetrahydropyrimidine-5-carboxylate.

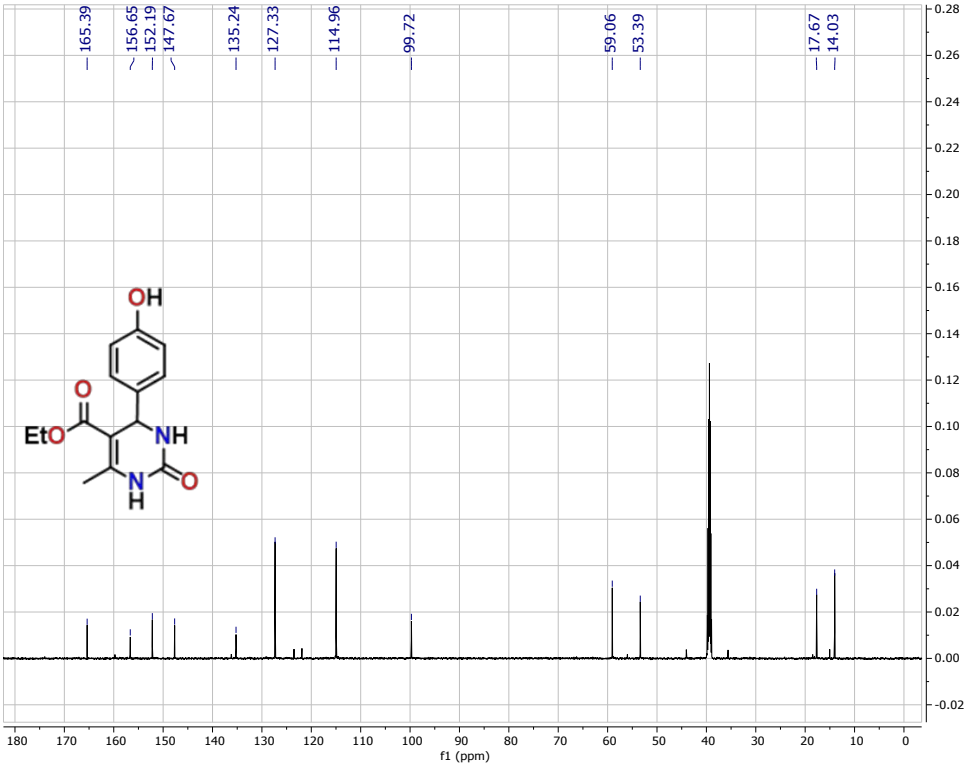

Figure S32. ^{13}C-NMR of the isolated ethyl 4-(4-hydroxyphenyl)-6-methyl-2-oxo-1,2,3,4-tetrahydropyrimidine-5-carboxylate.

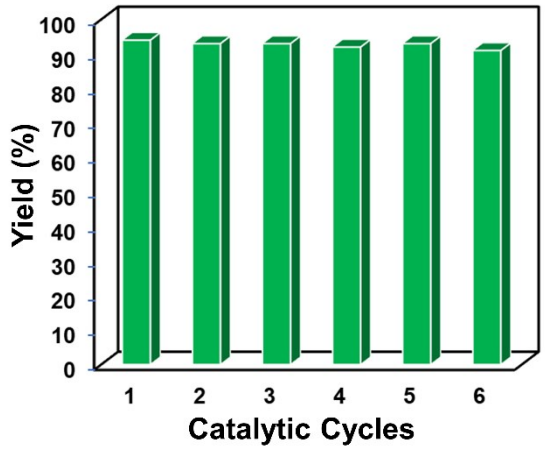

Figure S33. Recyclability of ADES-**1** up to 6 catalytic cycles for benzaldehyde conversion into Ethyl 6-methyl-2-oxo-4-phenyl-1,2,3,4-tetrahydropyrimidine-5-carboxylate.

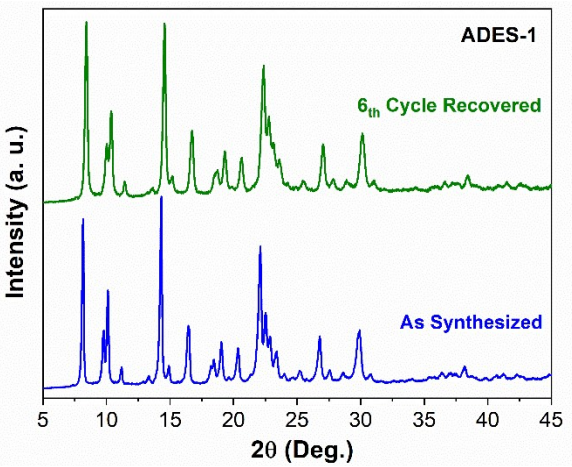

Figure S34. PXRD data of ADES-**1** recovered after 6 catalytic recycle for Biginelli reaction compared with PXRD data of as synthesized

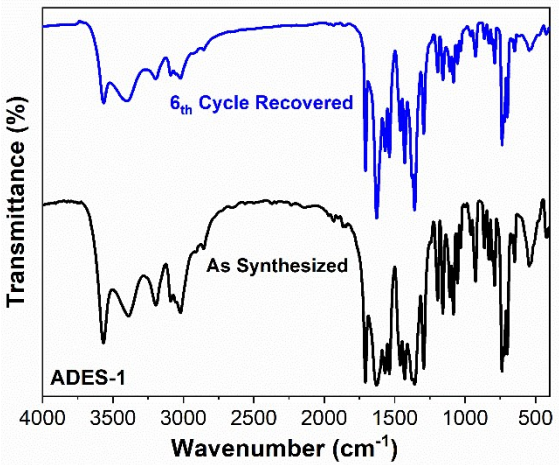

Figure S35. FTIR recorded for ADES-**1** (as synthesized and recovered after 6th catalytic recycle) dispersed in KBr pellets.

Table S2. Selected bond lengths and bond angles for ADES-**1** and ADES-**2**.

ADES-**1**			
Zn(1)-O(1)	2.0358(10)	Zn(1)-O(2)	2.0720(11)
Zn(1)-O(3)	2.1175(11)	Zn(1)-N(1)	2.1320(14)
Zn(1)-N(4)	2.1369(14)	Zn(1)-O(4)	2.3587(13)
O(1)-C(1)	1.2532(17)	N(2)-N(3)	1.3742(19)
O(2)-C(1)	1.2428(17)	N(2)-C(14)	1.358(2)
O(3)-C(8)	1.269(2)	O(4)-C(8)	1.2413(19)
N(3)-C(15)	1.268(2)	N(4)-C(17)	1.3397(19)
O(1)-Zn(1)-O(2)	124.29(4)	O(1)-Zn(1)-O(3)	146.99(4)
O(2)-Zn(1)-O(3)	88.68(5)	O(1)-Zn(1)-N(1)	87.58(5)
O(2)-Zn(1)-N(1)	91.71(5)	O(3)-Zn(1)-N(1)	93.58(5)
O(1)-Zn(1)-N(4)	87.38(5)	O(2)-Zn(1)-N(4)	90.29(5)
O(3)-Zn(1)-N(4)	91.20(5)	N(1)-Zn(1)-N(4)	174.86(5)
O(1)-Zn(1)-O(4)	88.41(4)	O(2)-Zn(1)-O(4)	147.30(4)
O(3)-Zn(1)-O(4)	58.65(4)	N(1)-Zn(1)-O(4)	89.19(5)
N(4)-Zn(1)-O(4)	91.69(5)	O(2)-C(1)-O(1)	125.41(13)
O(4)-C(8)-O(3)	122.62(14)	---	---
ADES-**2**			
Cd(1)-O(1)	2.2982(19)	Cd(1)-O(2)	2.3091(19)
Cd(1)-O(3)	2.4042(19)	Cd(1)-N(1)	2.302(2)
Cd(1)-N(4)	2.316(2)	Cd(1)-O(4)	2.401(2)
O(1)-C(1)	1.248(3)	N(2)-N(3)	1.380(3)
O(2)-C(1)	1.256(3)	N(2)-C(14)	1.347(4)
O(3)-C(8)	1.243(3)	O(4)-C(8)	1.248(3)
N(3)-C(15)	1.281(4)	O(7)-C(14)	1.254(4)
O(1)-Cd(1)-O(2)	126.85(7)	O(1)-Cd(1)-O(3)	136.14(7)
O(2)-Cd(1)-O(3)	96.78(7)	O(1)-Cd(1)-N(1)	95.99(8)
O(2)-Cd(1)-N(1)	85.89(7)	O(3)-Cd(1)-N(1)	90.92(7)
O(1)-Cd(1)-N(4)	89.67(8)	O(2)-Cd(1)-N(4)	84.78(8)
O(3)-Cd(1)-N(4)	90.10(8)	N(1)-Cd(1)-N(4)	170.67(8)
O(1)-Cd(1)-O(4)	82.19(7)	O(2)-Cd(1)-O(4)	150.92(7)
O(3)-Cd(1)-O(4)	54.15(7)	N(1)-Cd(1)-O(4)	93.25(10)
N(4)-Cd(1)-O(4)	94.86(10)	O(1)-C(1)-O(2)	122.9(2)
O(3)-C(8)-O(4)	122.7(2)	---	---

Table S3. Details of hydrogen bonding interactions observed in ADES-**1** and ADES-**2**.

D-H···A	d(H···A) (Å)	d(D···A) (Å)	∠D-H···A (°)
ADES-**1**			
N2-H2A···O8[1]	1.93	2.778 (3)	168
O8-H8A···O3[2]	1.96	2.807(4)	171
O8-H8A···O5[3]	2.15	2.939 (4)	170
C20-H20···O6[4]	2.39	3.053 (5)	126
ADES-**2**			
N2-H2C···O9[1]	2.25	3.067(5)	154
C11-H11···O9[1]	2.46	3.295(5)	146
C19-H19···O2[2]	2.54	3.137(3)	121
C22-H22···O3[3]	2.40	3.220(5)	145
Symmetry code: 1. 1+x,y,-1+z 2. 2-x,2-y,-z 3. -1+x,-1+y,z			

References:

S1. B. Parmar, Y. Rachuri, K. K. Bisht, R. Laiya and E. Suresh, Mechanochemical and Conventional Synthesis of Zn(II)/Cd(II) Luminescent Coordination Polymers: Dual Sensing Probe for Selective Detection of Chromate Anions and TNP in Aqueous Phase, *Inorg. Chem.,* 2017, **56**, 2627-2638.

S2. *APEX2*, v. 2014.7-1; Bruker AXS: Madison, WI, 2014.

S3. *SAINT*, v. 8.34A; Bruker AXS: Madison, WI, 2013.

S4. *SADABS*, v. 2014/3; Bruker AXS: Madison, WI, 2013.

S5. *SHELXTL*, v. 6.14; Bruker AXS: Madison, WI, 2000.

S6. A. L. Spek, PLATON SQUEEZE: a tool for the calculation of the disordered solvent contribution to the calculated structure factors, *Acta Crystallogr., Sect. C: Struct. Chem.,* 2015, **71**, 9-18.

S7. S. -Y. Zhao, Z. -Y. Chen, N. Wei, L. Liu and Z. -B. Han, Highly Efficient Cooperative Catalysis of Single-Site Lewis Acid and Brønsted Acid in a Metal–Organic Framework for the Biginelli Reaction, *Inorg. Chem.,* 2019, **58**, 7657-7661.

S8. A. Verma, D. De, K. Tomar and P. K. Bharadwaj, An Amine Functionalized Metal–Organic Framework as an Effective Catalyst for Conversion of CO_2 and Biginelli Reactions, *Inorg. Chem.,* 2017, **56**, 9765-9771.

S9. J. C. M. Willig, G. Granetto, D. Reginato, F. R. Dutra, E. F. Poruczinski, I. M. de Oliveira, H. A. Stefani, S. D. de Campos, E. A. de Campos, F. Manarin and G. V. Botteselle, A comparative study between $Cu(INA)_2$-MOF and $[Cu(INA)_2(H_2O)_4]$ complex for a click reaction and the Biginelli reaction under solvent-free conditions, *RSC Adv.,* 2020, **10**, 3407-3415.